

Synthesis and biological evaluation of 6H-1-benzopyrano[4,3-b]quinolin-6-one derivatives as inhibitors of colon cancer cell growth

Tie-Ling Li¹, Hai-Feng Guo², Fu-Juan Li³, Zhi-Guo Sun² and Heng-Chun Zhang²

¹Department of Pathology, MuDanJiang Medical University, Mudanjiang 157 011, China; ²Department of General Surgery, The affiliated Red Hospital of Mudanjiang Medical University, Mudanjiang 157 011, China; ³Department of Pathogenic Biology and Immunology Laboratory, MuDanJiang Medical University, Mudanjiang 157 011, China.

Article Info

Received: 12 June 2015
Accepted: 2 July 2015
Available Online: 2 August 2015
DOI: 10.3329/bjp.v10i3.23645

Cite this article:

Li TL, Guo HF, Li FJ, Sun ZG, Zhang HC. Synthesis and biological evaluation of 6H-1-benzopyrano[4,3-b]quinolin-6-one derivatives as inhibitors of colon cancer cell growth. Bangladesh J Pharmacol. 2015; 10: 660-71.

Abstract

A convenient synthesis of 6H-1-benzopyrano[4,3-b]quinolin-6-one derivatives was reported using 4-chloro-2-oxo-2H-chromene-3-carbaldehyde with different aromatic amines using silica sulfuric acid. The compounds were tested for their anticancer activity against colon (HCT-116 and S1-MI-80), prostate (PC3 and DU-145), breast (MCF-7 and MDAMB-231) cancer cells. These compounds showed more selectivity and potent cytotoxic activity against colon cancer cells. **3c** was tested against five other colon cancer cell lines (HT-29, HCT-15, LS-180, LS-174, and LoVo), which had similar cytotoxicity and selectivity. **3c** did not induce PXR-regulated ABCB1 or ABCG2 transporters. In fact, **3c** induced cytotoxicity in HEK293 cells over expressing ABCB1 or ABCG2 to the same extent as in normal HEK293 cells. It was cytotoxic approximately 3- and 5-fold to resistant colon carcinoma S1-MI-80 cells. **3c** also produced concentration-dependent changes in HCT-116 colon cancer cells, in mitochondrial membrane potential, leading to apoptosis, and sub-micromolar concentrations caused chromosomal DNA fragmentation.

Introduction

Coumarin is a fragrant organic chemical compound in the benzopyrone chemical class isolated from different plant sources (Geissman 1962; Harborne, 1988a; Harborne 1988b) and has various pharmacological activities. For example, the coumarin nucleus is present in a number of potential drug molecules such as nonpeptidic HIV protease inhibitors, (Thaisrivongs et al., 1996) topoisomerase II (Rappa et al., 2000) and tyrosine kinase inhibitors (Yang 1999).

Alternatively quinolines and their derivatives are known to have several applications in drugs and pharmaceuticals. A combination of benzopyran or chromen with a quinoline moiety in a single molecule, for example, 6H-chromeno[4,3-b]quinoline (Vu

et al., 2007; Hegab et al., 2007) or 1-benzopyrano[3,4-f]quinoline (Tabakovic et al., 1983) have also been identified for the promising bioactive molecules.

The combination of quinoline and coumarin in a single molecule, for example, 6H-1-benzopyrano[4,3-b]quinolin-6-one (Tabakovic et al., 1987; Mulakayala et al., 2012) is acknowledged as a separate class of heterocycle. It can be used as a model for the detection of bioactive molecules is not common. By knowing the cytotoxicities of coumarins and chromeno[4,3-b]quinoline derivatives (Ajdini et al., 1984), we hypothesized that design of small molecules based on 6H-1-benzopyrano[4,3-b]quinolin-6-one might show anticancer properties.

Herein we report the synthesis of a number of 6H-1-benzopyrano[4,3-b]quinolin-6-one derivatives along

with the *in vitro* anticancer properties of the compounds synthesized.

Materials and Methods

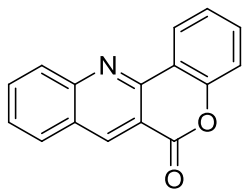
Chemistry

Chemicals and reagents were purchased either from Sigma or Merck, and all reagents were of analytical reagent grade. Thin-layer chromatography (TLC) was performed on Merck silica gel 60 F₂₅₄ plates and visualized under UV light. ¹H NMR spectra were recorded with Varian Mercury Plus 400 MHz instrument. ¹³C NMR spectra were recorded with a Varian Gemini 100 MHz instrument. All the chemical shifts are reported in μ (ppm) using TMS as an internal standard. Multiplicity is indicated by one or more of the following abbreviations: s (singlet), d (doublet), t (triplet), q (quartet), m (multiplet), br (broad); the coupling constants (J) correspond to the order of the multiplicity assignment. Mass spectra were recorded with a PE Sciex model API 3000 instrument. All the reactions were carried out under nitrogen atmosphere.

General procedure for the preparation of 6H-chromeno[4,3-b]quinolin-6-one (3a-j)

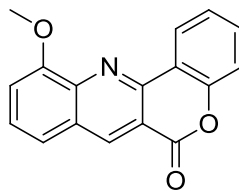
A solution of 4-chloro-2-oxo-2H-chromene-3-carbaldehyde (1 mmol) (Bairagi et al., 2009) and aromatic amine (1.5 mmol) in ethanol (5 mL) was added to amberlyst 15 (10 mol%). The reaction was refluxed for 2 hours and after completion of the reaction the reaction mixture was filtered to remove the catalyst. The filtrate was concentrated and the residue was purified by flash chromatography (n-hexane/ethyl-acetate 3:1) to afford the desired product.

6H-Chromeno[4,3-b]quinolin-6-one (3a)



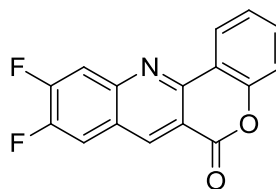
white solid; mp 224–227°C; ¹H NMR (400 MHz, DMSO-d₆): μ 9.34 (s, 1H), 8.65 (dd, J = 7.5 and 1.5 Hz, 1H), 8.30 (d, J = 8.1 Hz, 1H), 8.21 (d, J = 8.7 Hz, 1H), 8.03–8.05 (m, 1H), 7.64–7.74 (m, 2H), 7.45–7.49 (m, 2H); ¹³C NMR (100 MHz, DMSO-d₆): μ 160.7, 152.7, 150.4, 149.4, 141.2, 134.1, 133.0, 130.2, 129.0, 128.0, 127.3, 125.2, 125.0, 119.6, 117.6, 116.4; MS (ES mass): m/z 248 (M+1, 100%); HRMS: calcd for C₁₆H₁₀NO₂: 248.0702, found 248.0701.

11-Methoxy-6H-chromeno[4,3-b]quinolin-6-one (3b)



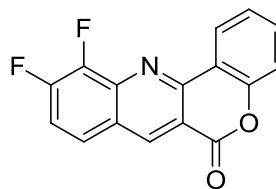
white solid; mp 234–236°C; ¹H NMR (400 MHz, DMSO-d₆): δ 9.1 (s, 1H), 8.85 (dd, J = 7.5 and 1.3 Hz, 1H), 7.56–7.62 (m, 3H), 7.38–7.45 (m, 2H), 7.24 (d, J = 5.7 Hz, 1H), 4.15 (s, 3H); ¹³C NMR (100 MHz, CDCl₃): δ 160.6, 153.2, 152.3, 150.0, 136.1, 129.7, 129.6, 127.7, 127.1, 126.5, 125.8, 124.3, 122.0, 110.1, 114.8, 112.2, 56.1; MS (ES mass): m/z 278 (M+1, 10%); HRMS: calcd for C₁₇H₁₂NO₃: 278.0815, found 278.0817.

9,10-Difluoro-6H-chromeno[4,3-b]quinolin-6-one (3c)



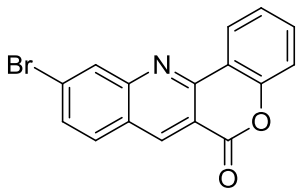
white solid; mp 252–255°C; ¹H NMR (400 MHz, CDCl₃): μ 9.23 (s, 1H), 8.84 (dd, J = 8.1 and 1.5 Hz, 1H), 7.83–7.87 (m, 1H), 7.63–7.67 (m, 1H), 7.41–7.56 (m, 3H); ¹³C NMR (100 MHz, CDCl₃): μ 160.9, 152.8, 150.1, 140.2, 140.1, 132.8, 125.3, 125.2, 119.2, 117.5, 115.9, 115.7, 114.5, 114.4, 114.3, 114.2; MS (ES mass): m/z 284 (M+1, 100%). HRMS: calcd for C₁₆H₈F₂NO₂: 284.0465, found: 284.04653.

10,11-Difluoro-6H-chromeno[4,3-b]quinolin-6-one (3d)



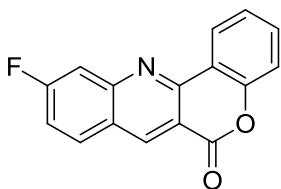
white solid; mp 257–260°C; ¹H NMR (400 MHz, DMSO-d₆): μ 9.46 (s, 1H), 8.62 (dd, J = 7.5 and 1.3 Hz, 1H), 8.24–8.28 (m, 1H), 7.84–7.91 (m, 1H), 7.75–7.70 (m, 1H), 7.41–7.50 (m, 2H); ¹³C NMR (100 MHz, CDCl₃): μ 160.7, 152.8, 150.5, 141.0, 133.1, 125.6, 125.4, 125.3 (2C), 125.2, 125.1, 124.8, 119.0, 118.7, 118.5, 117.3; MS (ES mass): m/z 284 (M+1, 100%); HRMS: calcd for C₁₆H₇F₂NO₂: 284.0486, found 284.0478.

10-Bromo-6H-chromeno[4,3-b]quinolin-6-one (3e)



White solid; mp 245-247°C; ^1H NMR (400 MHz, CDCl_3): μ : 9.21 (s, 1H), 8.74 (dd, $J = 8$ and 1.5 Hz, 1H), 8.44 (s, 1H), 7.88 (d, $J = 8.7$ Hz, 1H), 7.72 (dd, $J = 8.7$ and 1.5 Hz, 1H), 7.61-7.65 (m, 1H), 7.38-7.47 (m, 2H); ^{13}C NMR (100 MHz, DMSO-d_6): μ 161.1, 152.9, 150.5, 141.2, 132.9, 132.7, 131.9, 131.8, 131.3, 130.4, 125.9, 125.5, 125.2, 117.5, 115.9, 110.1; MS (ES mass): m/z 327.1 (M+2, 100%); HRMS: calcd for $\text{C}_{16}\text{H}_9\text{BrNO}_2$: 327.2545, found 327.2541.

10-Fluoro-6H-chromeno[4,3-b]quinolin-6-one (3f)



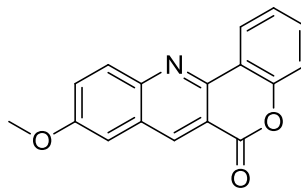
white solid; mp 234-237°C; ^1H NMR (400 MHz, CDCl_3): μ 9.20 (s, 1H), 8.76 (dd, $J = 8.1$ and 1.5 Hz, 1H), 8.01-8.05 (m, 1H), 7.85 (dd, $J = 9.8$ and 2.3 Hz, 1H), 7.58-7.65 (m, 1H), 7.38-7.48 (m, 3H); ^{13}C NMR (100 MHz, DMSO-d_6): μ 160.6, 153.1, 151.5, 150.6, 141.6, 133.5, 125.5, 125.2, 124.9, 119.5, 118.9, 118.6, 117.8, 116.1, 112.8, 112.6; MS (ES mass): m/z 266.2 (M+1, 100%); HRMS: calcd for $\text{C}_{16}\text{H}_9\text{FNO}_2$: 266.2021, found 266.2018.

9-Fluoro-6H-chromeno[4,3-b]quinolin-6-one (3g)



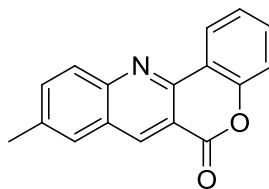
white solid; mp 224-226°C; ^1H NMR (400 MHz, CDCl_3): μ 9.18 (s, 1H), 8.78 (dd, $J = 8.1$ and 1.5 Hz, 1H), 8.26-8.27 (m, 1H), 7.58-7.73 (m, 3H), 7.41-7.46 (m, 2H); ^{13}C NMR (100 MHz, DMSO-d_6): μ 160.9, 152.8, 150.3, 149.4, 141.3, 134.1, 133.0, 130.2, 129.1, 127.8, 127.4, 125.2, 125.1, 119.6, 117.6, 116.3; m/z 266.4 (M+1, 100%); HRMS: calcd for $\text{C}_{16}\text{H}_9\text{FNO}_2$: 266.3032, found 266.3028.

9-Methoxy-6H-chromeno[4,3-b]quinolin-6-one (3h)



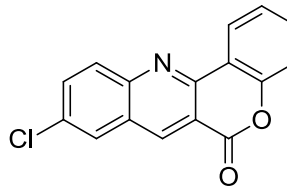
white solid; mp 229-231°C; ^1H NMR (400 MHz, CDCl_3): μ 9.2 (s, 1H), 8.77 (dd, $J = 9.9$ and 1.5 Hz, 1H), 8.13 (d, $J = 9.1$ Hz, 1H), 7.54-7.60 (m, 2H), 7.38-7.44 (m, 2H), 7.22 (d, $J = 2.7$ Hz, 1H), 3.98 (s, 3H); ^{13}C NMR (100 MHz, TFA): μ 159.5, 153.7, 151.5, 147.5, 142.1, 138.8, 134.6, 134.5, 127.1, 124.7, 124.1, 122.0, 121.7, 118.8, 105.8, 105.5, 58.5; MS (ES mass): m/z 278.1 (M+1, 100%); HRMS: calcd for $\text{C}_{17}\text{H}_{12}\text{NO}_3$: 278.0815, found 278.0813.

9-Methyl-6H-chromeno[4,3-b]quinolin-6-one (3i)

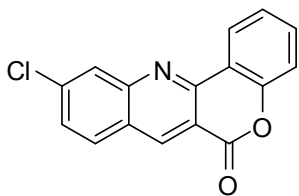


white solid; mp 234-236°C; ^1H NMR (400 MHz, CDCl_3): μ 9.11 (s, 1H), 8.76 (dd, $J = 8.1$ and 1.5 Hz, 1H), 8.13 (d, $J = 8.3$ Hz, 1H), 7.73-7.75 (m, 2H), 7.55-7.57 (m, 1H), 7.37-7.44 (m, 2H), 2.58 (s, 3H); ^{13}C NMR (100 MHz, DMSO-d_6): μ 160.8, 152.7, 150.7, 149.5, 145.0, 140.8, 132.88, 130.2, 129.8, 128.1, 125.7, 125.2, 124.5, 119.7, 117.6, 115.5, 22.2; MS (ES mass): m/z 262.2 (M+1, 100%); HRMS: calcd, for $\text{C}_{17}\text{H}_{12}\text{NO}_2$: 262.0869, found 262.0867.

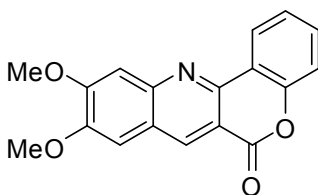
9-Chloro-6H-chromeno[4,3-b]quinolin-6-one (3j)



white solid; mp 242-244°C; ^1H NMR (400 MHz, CDCl_3): μ 9.0 (s, 1H), 8.75 (dd, $J = 7.5$ and 1.5 Hz, 1H), 8.17-8.21 (d, $J = 9.3$ Hz, 1H), 8.1 (s, 1H), 7.86 (dd, $J = 9.1$ and 2.5 Hz, 1H), 7.58-7.63 (m, 1H), 7.38-7.45 (m, 2H); ^{13}C NMR (100 MHz, CDCl_3): μ 160.8, 152.4, 149.6, 149.1, 139.8, 134.1, 133.2, 132.5, 131.1, 127.6, 127.5, 125.1, 125.0, 119.1, 117.3, 116.3; MS (ES mass): m/z 282.2 (M+1, 100%); HRMS: calcd for $\text{C}_{16}\text{H}_9\text{ClNO}_2$: 282.0244, found 282.0242.

10-Chloro-6H-chromeno[4,3-b]quinolin-6-one (3k)

White solid; m.p. 243 -245°C; ¹H NMR (400 MHz, CDCl₃): δ 9.05 (s, 1H), 8.70 (d, *J* = 6.7 Hz, 1H), 8.12 (d, *J* = 9.1 Hz, 1H), 7.93 (d, *J* = 1.8 Hz, 1H), 7.82 (dd, *J* = 8.9 Hz and 2.1, 1H), 7.55 - 7.60 (m, 1H), 7.34 - 7.42 (m, 1H); ¹³C NMR (100 MHz, CDCl₃): δ 161.0, 152.8, 150.6, 149.5, 140.0, 134.3, 133.6, 132.7, 131.2, 127.8, 127.7, 125.3, 125.1, 119.4, 117.5, 116.5; MS (ES mass): *m/z* 282.2 (M+1, 100%); HRMS calcd for C₁₆H₈O₂NCl, 281.0242 found 281.0246

9,10-Dimethoxy-6H-chromeno[4,3-b]quinolin-6-one (3l)

Yellow solid; mp 291-294 °C, ¹H NMR (400 MHz, CDCl₃): δ 8.94 (s, 1H), 8.66 (d, *J* = 7.7 Hz, 1H), 7.53 (t, *J* = 7.5 Hz, 1H), 7.47 (s, 1H), 7.37 (dd, *J* = 7.8 and 14.3 Hz, 2H), 7.11 (s, 1H), 4.10 (s, 3H), 4.03 (s, 3H); ¹³C NMR (100 MHz, CDCl₃): δ 161.7, 156.1, 152.5, 150.8, 149.3, 148.1, 137.8, 131.7, 124.8, 124.7, 123.6, 120.1, 117.4, 114.2, 107.6, 105.6, 56.6, 56.4; MS (ES mass): *m/z* 307.2 (M+1, 100%); HRMS calcd for C₁₈H₁₃O₄N, 307.0840 found 307.0834.

Biology

DMEM media, 0.25% trypsin, propidium iodide, paclitaxel, buffers, and reagents were purchased from VWR (VWR International Inc., Suwanee, GA). MitoTracker Red and Alexa Fluor 488 annexin V kits for flow cytometry were purchased from Life Sciences (Molecular Probes Inc., Invitrogen, Eugene, OR). DMSO and RIF were purchased from Sigma.

Cell culture

Colon carcinoma cell lines [HCT-116, HCT-15, HT-29, Lovo, LS-180, LS-174, S1 (a clone of LS174T cells)] and prostatic cancer cell lines [DU-145 and PC-3] and breast carcinoma cells [MDA-MB-231 and MCF-7] were grown as adherent monolayers in flasks with Dulbecco's Modified Eagle Medium (DMEM) supplemented with 10% fetal bovine serum (FBS) in a humidified incubator containing 5% CO₂ at 37°C. A G482 mutant ABCG2-overexpressing, drug-resistant colon cancer cell line, S1-M1-80, was

maintained in medium with 80 μM mitoxantrone (Miri et al., 2011; Robey et al., 2001). The assay media for PXR transactivation assays included phenol red-free DMEM (Lonza) supplemented with 5% charcoal/dextran-treated FBS (HyClone) and the other additives.

PXR transactivation assay

HepG2 cells were transfected with pcDNA3-hPXR and CYP3A4-luc plasmids using FuGENE 6 (Promega). After 24 hours of transfection in growth media, 10,000 cells were plated into wells of 96-well culture plates (PerkinElmer), and treated with DMSO, RIF, or **3c** for an additional 24 hours. At 48 hours of transfection, a luciferase assay was performed to measure luminescence using the Neolite Reporter Gene Assay System (PerkinElmer) and a FLUOstar Optima microplate reader (BMG Labtech). Normalized CYP3A4 promoter activity was expressed as fold induction over the DMSO control. Cell viability was measured in parallel by CellTiter-Glo luminescent assays (Promega), which determine the number of metabolically active cells by quantifying the ATP present. Luminescence was measured with a FLUOstar Optima plate reader (BMG Labtech).

Cell cytotoxicity as determined by MTT assays and morphological analysis

The MTT assay (Carmichael et al., 1987) was used to determine cytotoxicity of the compounds to the following cells: HCT-116, HCT-15, HT-29, LS-180, LS-174, Lovo, S1, DU-145, PC-3, MDA-MB-231 and MCF-7. Briefly, the cells were harvested with trypsin and suspended at a final concentration of 5 × 10³ cells/well. Cells were seeded (180 μL/well) into 96-well multiplates. Different concentrations of 6H-1-benzopyrano [4,3-b]quinolin-6-one derivatives (20 μL/well) were added. After 72 hours of incubation, 20 μL of MTT solution (4 mg/mL) was added in each well, and the plates were incubated further 4 hours, allowing the viable cells to convert the yellow-colored MTT into dark-blue formazan crystals. Subsequently, the medium was removed, and DMSO (100 μL) was added in each well to dissolve the formazan crystals. The absorbance was determined at 570 nm with an OPSYS microplate Reader (DYNEX Technologies, Inc., Chantilly, VA, USA). The means ± SD concentrations were calculated from at least three experiments performed in triplicate. The IC₅₀ values were calculated from survival curves using the Bliss method. At 68 hours, cells with or without treatment were photographed by use of an inverted microscope (Olympus, BX53F) with fluorescent lamps and digital cameras. The data were acquired and analyzed by CellSens software.

Mitochondrial membrane potential and DNA fragmentation analysis

Mitochondrial membrane potential and apoptosis

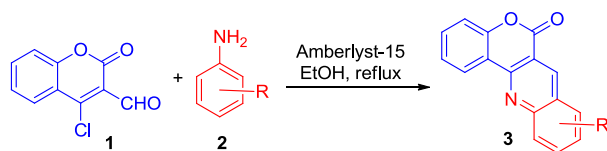
were measured for colon cancer HCT-116 cells using MitoTracker Red and Alexa Fluor 488 annexin V kits for flow cytometry (Molecular Probes Inc., Invitrogen, Eugene, OR). Briefly, apoptosis was induced by exposing HCT-116 cells (seeded in 6 well-plates) with or without 3C at 1 or 10 μM concentrations for 4 hours. Equal amounts of cells were harvested, and, to each mL of cells, 4 μL of 10 μM working solution of MitoTracker Red was added. Cells were stained at 37°C for 30 min in an atmosphere of 5% CO_2 . The cells were washed with PBS and suspended in 100 μL of 1X annexin-binding buffer, to which 5 μL of Alexa Fluor 488 annexin V was added. Cells were incubated for an additional 15 min, after which 400 μL of 1X annexin-binding buffer was added. The stained cells were counted by flow cytometry, measuring the fluorescence at 530 nm and 585 nm (BD FACSCalibur Flow Cytometer using FlowJo FACS data analysis software).

A characteristic feature of apoptosis is induction of oligonucleosomal DNA fragmentation by cytotoxic compounds, which activate nucleases that degrade the higher-order chromatin structure of DNA into mono- and oligonucleosomal DNA fragments (Henkels and Turchi, 1999; Wu et al., 2005). To establish the mode of action of 3C in colon cancer cytotoxicity, a DNA fragmentation assay was performed. Apoptotic degradation of DNA was analyzed by agarose gel electrophoresis. Briefly, HCT-116 cells were cultured in the presence of 3c (2.5 μM) for 6 hours. Genomic DNA was extracted from the cells by use of Promega Wizard Genomic DNA purification kits (Promega Corporation, Madison, WI) and resolved on 1% agarose gels at 40V for 4 hours. DNA was visualized by ethidium bromide staining and photographed.

Results and Discussion

Chemistry

To find the convenient procedure we investigated the cyclization of 4-chloro-2-oxo-2H-chromene-3-carbaldehyde (**1**) with aniline (**2**) using Amberlyst-15 resin as catalyst in ethanol under reflux (**Scheme-1**) for 2 hours which yielded 6H-1-benzopyrano[4,3-b]quinolin-6-one **3a** in 91% (Table I). Several amines



Scheme I: Synthetic scheme of 6H-1-benzopyrano[4,3-b]quinolin-6-one derivatives from 4-chloro-2-oxo-2H-chromene-3-carbaldehyde

were used for checking the compatibility of this method. All the amines including aromatic and substituted aromatic amines were well tolerated with the current methodology to yield the required products in good to excellent yields. Thus, the structures of the synthesized compounds are shown in Table I.

Biological evaluation

Growth curves, cell cytotoxicity, and morphological analysis for 6H-1-benzopyrano [4,3-b]quinolin-6-one derivative derivatives (3a-3l)

6H-1-benzopyrano[4,3-b]quinolin-6-one derivatives (3a-3l) were evaluated for cytotoxic effects on threetypes of cancer cells, that is, colon (HCT-116 and S1), prostate (PC3 and DU-145), breast (MCF-7 and MDAMB-231) cell lines. The 3-(4,5-dimethylthiazol-2-yl)-2,5-diphenyltetrazolium bromide (MTT) assay was used. All compounds were tested at concentrations ranging from 0.1 μM to 100 μM . The 50% minimum inhibitory concentrations (IC_{50}) are summarized in Table I.

6H-1-benzopyrano [4,3-b]quinolin-6-one derivatives (3a-3l) were exhibited variable degrees of growth inhibitory activity towards the three human cancer cell lines (Table I). Compound 3d, showed only a modest inhibitory activity ($\text{IC}_{50} >40 \mu\text{M}$) on the tested cells. Other compounds, with the exception of 3d, showed moderately more or less cytotoxic activity relative to 3c.

Compound 3c with a 9,10-difluoro substitution, was most effective against breast (MDAMB-231) cancer cells, with IC_{50} values ranging between 44 and 50 μM . A similar cytotoxic profile against colon cancer (HCT-116 and S1) and breast cancer cells was observed for 3f, which has a 10-fluoro substitution. Among the eight compounds studied, 3C, with a difluoro substitution on the 9 and 10 position of the 6H-1-benzopyrano [4,3-b]quinolin-6-one ring, showed selective and potent growth inhibition against colon cancer cells. The IC_{50} values of 3c against HCT-116 and S1 cells were 0.6 μM and 0.8 μM , respectively. Prostate cancer cells (PC-3 and DU-145) were also inhibited by 3c, with an IC_{50} values ranging from 0.8 μM to 1.2 μM . Further, 3c showed moderate growth inhibitory activity ($\text{IC}_{50} >10 \mu\text{M}$) against breast (MCF-7 and MDAMB-231) cancer cells. Overall, these results established that the 9,10-difluoro substitution is significant to the anticancer activity of 6H-1-benzopyrano [4,3-b]quinolin-6-one and that compound 3c was a promising candidate for further studies with colon cancer cells.

3c exhibits potent and selective cytotoxic activity on various colon cancer cells results of compound 3c on colon carcinoma cells encouraged us to expand our

Table I

Synthesis of a novel series of substituted 5-(aminomethylene)thiazolidine-2,4-diones^a

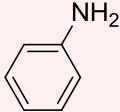
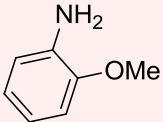
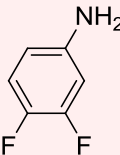
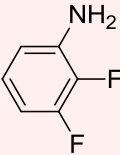
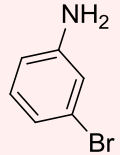
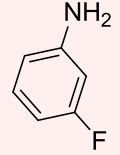
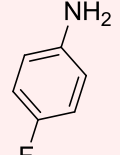
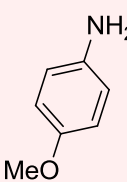
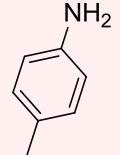
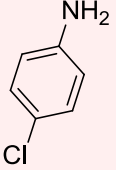
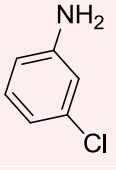
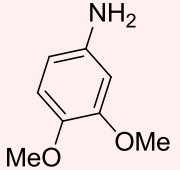
Entry	Amine (2)	Product	Yield (%) ^b
1		3a	92
2		3b	93
3		3c	81
4		3d	78
5		3e	84
6		3f	87
7		3g	82
8		3h	85
9		3i	92

Table I			
Synthesis of a novel series of substituted 5-(aminomethylene)thiazolidine-2,4-diones ^a (Cont.)			
Entry	Amine (2)	Product	Yield (%) ^b
10		3j	96
11		3k	96
12		3l	97

^aAll the reactions were performed using 4-chloro-2-oxo-2H-chromene-3-carbaldehyde **1** (1.0 mmol), aniline **2** (1.1 mmol) and amberlyst-15 (15 mol%), ethanol (10 vol.), reflux, 2-3 hours; ^bIsolated yields

Table II						
Activity of 6H-1-benzopyrano [4,3-b]quinolin-6-one derivatives against various cell lines						
Compound	Colon		Prostate		Breast	
	HCT-116	S1	PC3	DU-145	MCF-7	MDAMB-231
3a	48.6 ± 8.6	54.2 ± 9.8	65.2 ± 13.2	69.4 ± 12.4	76.5 ± 16.4	78.5 ± 14.2
3b	56.2 ± 11.3	61.2 ± 10.6	71.3 ± 11.2	71.9 ± 12.9	86.2 ± 14.3	82.1 ± 12.3
3c	1.6 ± 0.1	1.7 ± 0.1	0.9 ± 0.2	1.6 ± 0.6	7.6 ± 0.8	6.6 ± 0.4
3d	4.6 ± 0.4	3.8 ± 0.3	5.2 ± 0.5	6.4 ± 0.4	11.2 ± 1.1	13.2 ± 1.6
3e	82.5 ± 14.3	86.5 ± 15.6	93.2 ± 17.6	91.4 ± 16.3	74.6 ± 12.6	72.6 ± NA
3f	12.1 ± 3.2	12.9 ± 2.8	15.3 ± 5.3	16.2 ± 4.8	18.3 ± 5.3	17.6 ± NA
3g	13.5 ± 2.9	14.6 ± NA	21.6 ± 4.3	25.3 ± 4.3	17.6 ± 4.3	18.3 ± 5.3
3h	91.6 ± 12.4	93.5 ± 4.2	120.3 ± 18.3	114.6 ± 17.2	93.2 ± 14.2	91.3 ± 7.5
3i	86.3 ± 14.3	84.3 ± 15.2	95.6 ± 15.6	92.3 ± 14.3	72.3 ± NA	75.8 ± 12.9
3j	89.5 ± NA	95.8 ± 18.2	44.6 ± NA	87.3 ± 11.2	106.7 ± 19.4	110.5 ± 18.6
3k	85.4 ± 14.2	83.4 ± 7.4	111.4 ± 18.3	94.5 ± 14.6	58.4 ± 6.9	62.4 ± 4.6
3l	91.6 ± 12.7	72.8 ± 11.6	57.3 ± 15.8	53.7 ± 17.8	78.6 ± 16.2	71.6 ± 12.4

Cell survival assay was determined by the MTT assay. IC₅₀ values are represented as means ± SD of three independent experiments performed in triplicate. A mean IC₅₀ value of 100 mM was the cut off. NA, not assessed

studies to different types of colon cancer cells (HCT-15, HT-29, Lovo, LS-180, and LS-174). All these cancer cells were sensitive to 3c at concentrations ranging from μM 0.6

to 1.0 μM (Table II, Figure 1A and B). Notably, 3c was 10–15 fold more selective for inhibition of colon cancer cells relative to HEK293 cells (Figure 1A and B); 10–30

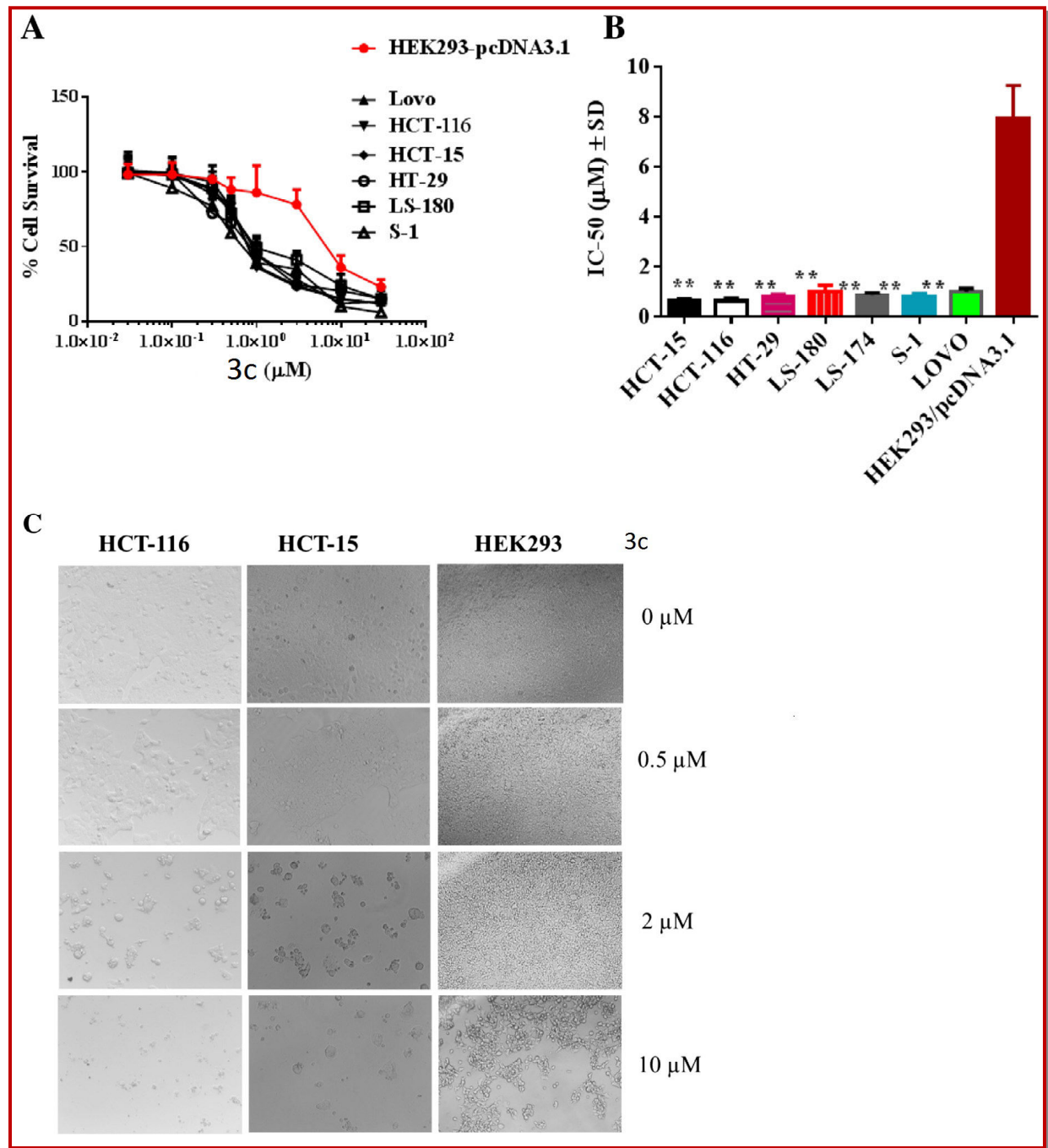


Figure 1: Cytotoxic effects of 3c

A) Survival of colon cancer cells S1, HCT-116, HCT-15, HT-29, Lovo, and LS-180 compared to that of human embryonic kidney cells, EK293/pcDNA3.1; B) IC₅₀ values of 3c for colon cancer cells S1, HCT-116, HCT-15, HT-29, Lovo, and LS-180 relative to human embryonic kidney cells (HEK293/pcDNA3.1). Cell survival was determined by the MTT assay. IC₅₀ values are represented as means \pm SD of three independent experiments performed in triplicate. Statistically, * $p < 0.05$; ** $p < 0.01$, colon cancer cells versus the HEK293/pcDNA3.1; C) Morphological analysis of the cytotoxic effects of 3c (0, 0.5, 2 and 10 M) on colon cancer cells, HCT-116 and HCT-15; prostate cancer cells, DU-145; and human embryonic kidney cells HEK-293, exposed for 68 hours, was made by microscopy at 20 \times . The cells were photographed for each triplicate treatment with an inverted microscope (Olympus, BX53F) with fluorescent lamps and digital cameras. A representative figure is shown for each treatment. The data were acquired and analyzed with Cell Sens software

Table II	
IC ₅₀ values for IND-2 inhibition of various colon cancer cell lines	
Colon cancer cells	IC ₅₀ ± SD (nM) 3c
HCT-15	670.6 ± 48.9
HCT-116	634.5 ± 120.1
HT-29	790.8 ± 103.5
LS-180	1023.5 ± 230.6
LS-174	874.6 ± 89.7
S1	798.3 ± 137.4
Lovo	993.8 ± 142.6

fold more selective for other cancer cells. (breast, prostate) (Table I); After 68 hours of treatment of HCT-

116, HCT-15, and HEK293 cells with 0, 0.5, 2, or 10 μ M 3c, morphological changes, complementing the cytotoxicity data, were evident in all the cells (Figure 1c shows representative images). In sum, the cytotoxic effect of 3c on colon cancer cells is particularly notable because of its selectivity and its IC₅₀ values of <1 μ M.

3C does not activate pregnane X receptor (PXR), is not a substrate of ABCB1 or ABCG2 transporters, and is cytotoxic to chemoresistant colon cancer cells

PXR is a ligand-dependent nuclear receptor involved in regulating the expression of ATP-binding cassette (ABC) transporters, including ABCB1 (a.k.a. P-glycoprotein) and ABCG2 (a.k.a. breast cancer resistance protein, BCRP) (Pondugula et al., 2009, Pondugula and Mani, 2013). Activation of PXR by xenobiotics leads to chemoresistance, concern in drug development and clinical therapy. The possible activation of PXR by 3C was examined with HepG2 cell-based reporter gene assays. Although rifampicin (RIF), an agonist of human

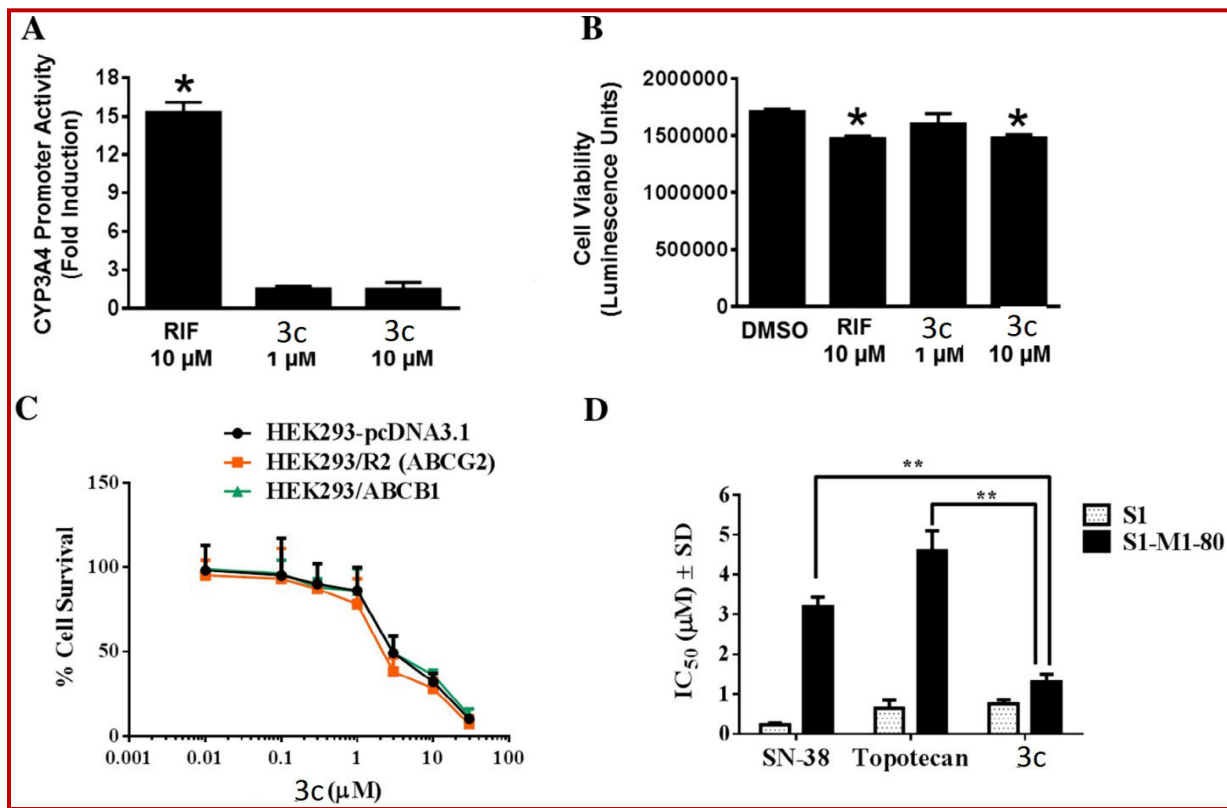


Figure 2: 3c does not induce human PXR transactivation of CYP3A4 promoter activity

A) CYP3A4 promoter activity was determined in HepG2 cells after transient cotransfection with pGL3-CYP3A4-luc reporter and pcDNA3-hPXR plasmids for 24 hours, followed by treatment with DMSO, RIF, or 3c for an additional 24 hours. The induction of CYP3A4 promoter activity was normalized as fold increase over the DMSO control. Data represent means \pm SD from three different experiments. Statistical significance ($*p < 0.05$) was determined with Student's *t* test by comparing the effects of RIF or 3c with DMSO; B) Effect of 3c on HepG2 cell viability. During the PXR transactivation studies, viability of HepG2 cells was determined simultaneously in parallel experiments with the Cell Titer-Glo luminescent cell viability assay kit and the data are expressed as luminescence units. Data represent the means \pm SD of triplicate determinations. Statistical significance ($*p < 0.05$) was determined with Student's *t* test by comparing the effects of RIF or 3c with DMSO; C) Effect of 3c on the survival of cells overexpressing ABCB1 or ABCG2. Effects of 3c, topotecan, and SN-38 on S1 and S1-M1-80 cells. MTT cytotoxicity assays were used to measure survival of HEK293/pcDNA3.1, HEK293/R2, HEK293/ABCB1, S1, and S1-M1-80 cells. Data points represent the means \pm SD of triplicate determinations. Representative results from three independent experiments, each performed in triplicate, are shown

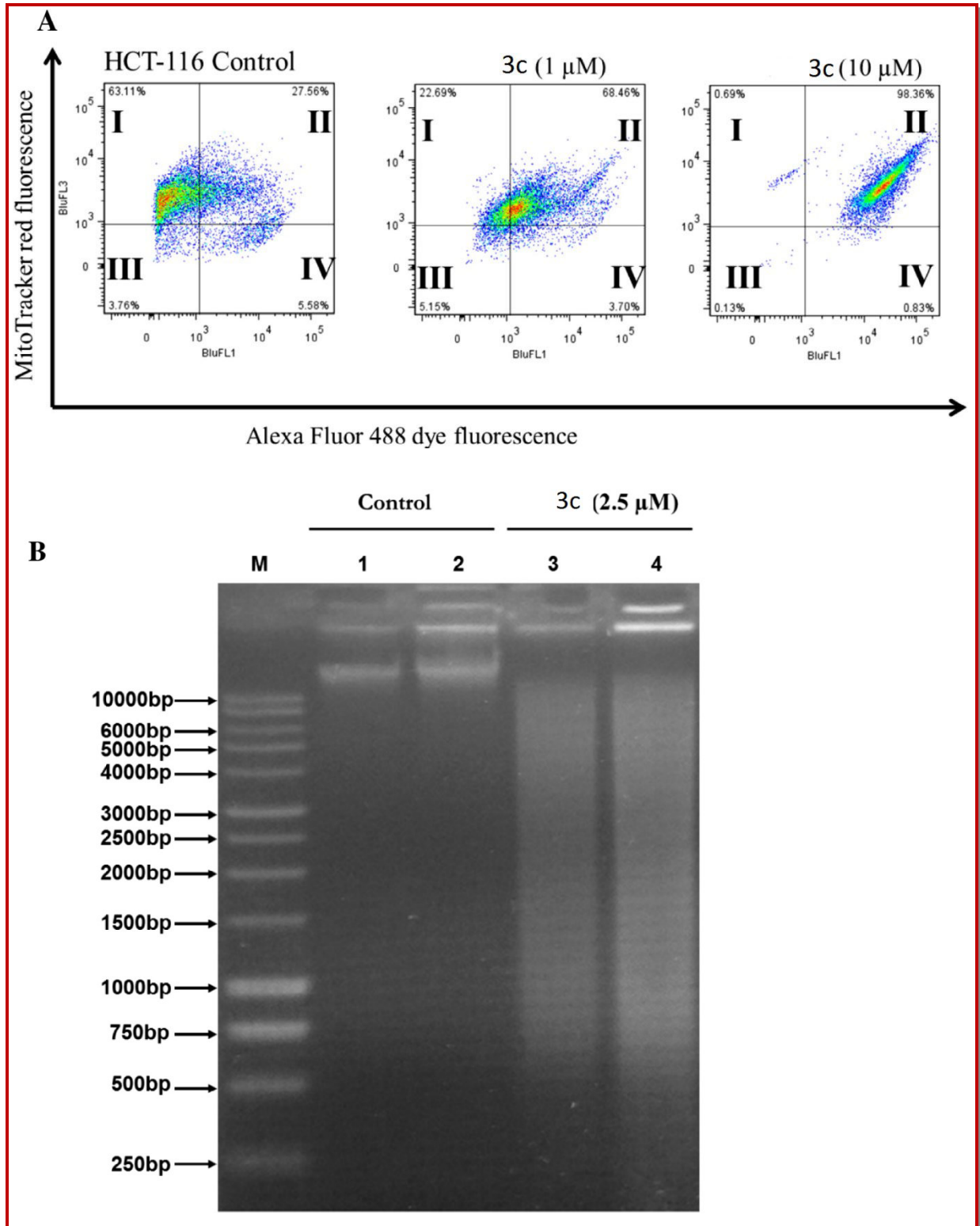


Figure 3: Effects of 3c on mitochondrial membrane potential and DNA fragmentation

A) HCT-116 cells in complete medium were exposed to 3c (0, 1, or 10 mM) for 4 hours. Cells were then treated with the reagents of the MitoTracker Red and Alexa Fluor 488 annexin V kits for flow cytometry. Representative results from two independent experiments, each performed in triplicate, are shown; B) 3c induced DNA damage in HCT-116 cells. Chromosomal DNA was extracted from HCT-116 cells and resolved on a 1% agarose gel at 40 V for 6 hours. Lane 1: 'M', Marker; lanes 2 and 3: untreated HCT cells, 500 ng and 1 μ g, respectively; lanes 4 and 5: HCT cells incubated with 3c (2.5 mM) for 6 hours

PXR, induced PXR transactivation of CYP3A4 promoter activity, **3c** at 1 or 10 μM did not affect PXR transactivation (Figure 2A), showing that **3c** does not activate PXR at concentrations cytotoxic to colon cancer cells and indicating that **3c** does not induce PXR-mediated drug resistance in cancer cells. Similar to RIF, **3c** at 10 μM was marginally cytotoxic, although **3c** at 1 μM was non-cytotoxic (Figure 2B), showing that the lack of effect of **3c** on PXR was not due to cytotoxicity.

Multi-drug resistance (MDR) factors, such as ABCB1 and ABCG2 transporters, present limitations for the development of anticancer agents. (Perin et al., 2011) These transporters are expressed in a variety of solid and hematological malignancies, where they are involved in the efflux of various therapeutic drugs, leading to MDR. Ideally, drugs that are not substrates for these transporters are preferred as anticancer agents. **3c** was screened against ABCB1- and ABCG2-over-expressing cells, and its effects were compared with positive controls paclitaxel and mitoxantrone, respectively. There was no substantial resistance to **3c** in ABCB1- or ABCG2-overexpressing cells, as all the cells were sensitive at similar concentrations of **3c** (Figure 2C), indicating that **3c** is not a substrate for ABCB1 and ABCG2 transporters. These results support our PXR analysis (Figure 2A). Additionally, the cytotoxic potential of **3c** was evaluated for a G482 mutant ABCG2-over-expressing, drug-resistant colon cancer cell line, S1-M1-80. S1-M1-80 cells showed significant resistance ($p < 0.001$) to SN-38, an active metabolite of irinotecan and topotecan (Figure 2D). **3c**, however, inhibited the resistant S1-M1-80 cells 3-5 fold more potently ($p < 0.001$) than SN-38 and topotecan (Figure 2D). This could be because: (a) **3c** did not interact with ABCG2 transporters, was not effluxed by resistant S1-M1-80 cells, and maintained its cytotoxic concentration, or (b) **3c** blocked the ABCG2 transporters and retained its cytotoxic potential in resistant S1-M1-80 cells. If the second reason is true, **3c** may be beneficial in combination chemotherapy against colorectal and other tumors with agents that are substrates of ABCG2 transporters. However, further mechanistic experiments including ATPase, photo-affinity labeling assays, and combination chemotherapy are necessary to confirm the interactions of **3c** with ABCB1 and ABCG2 transporters.

3c induces reduces mitochondrial membrane potential and causes apoptosis and DNA fragmentation in coloncancer cells

Inappropriately regulated apoptosis is implicated in cancer. Whereas, mitochondrial dysfunction is involved in signaling processes that initiate apoptotic events, loss of membrane asymmetry, cytochrome c, and other apoptogenic factors

released from mitochondria initiate apoptotic cell death. In the process of apoptosis, phosphatidylserine (PS), otherwise located on the cytoplasmic surface, is displaced from the inner to the outer leaflet of the plasma membrane. The extracellular exposed PS has high affinity for binding to the human vascular anticoagulant, annexin V, a 35-36 kDa, Ca^{2+} -dependent, phospholipid-binding protein. This principle is used to determine the binding of annexin V, labeled with a fluorophore or biotin, to exposed PS on the outer leaflet and thereby to identify apoptotic cells. (Koopman et al., 1994) Live cells, 63.11% of untreated HCT-116 cells with intact mitochondrial membranes, are seen in quadrant I of Figure 3A. Of these cells, 27.6% had a loss in mitochondrial membrane potential and had started the process of apoptosis. Treatment with **3c**, even at 1 μM , for 4 hours produced a significant loss ($p < 0.01$) of membrane potential in 68.46% of the cells, as seen in quadrant II of Figure 3A. At 10 μM , **3c** treatment for 4 h showed that almost all the cells (98.36%) had no or low mitochondrial membrane potential and thus were primed to undergo apoptosis (quadrant II of Figure 3A). These data show that **3c** produces concentration-dependent decreases in mitochondrial potential of HCT-116 colon cancer cells, leading to apoptosis.

The extent of **3c**-induced DNA damage in HCT-116 colon cancer cells was assessed by chromosomal DNA fragmentation. Treatment with 2.5 μM **3c** for 6 h led to fragmentation of chromosomal DNA (Figure 3B). In contrast, chromosomal DNA of untreated cells was intact. These results indicate that **3c** induces DNA breakage at multiple positions across chromosomal DNA, leading to apoptosis.

Conclusion

The present study describes the synthesis of 6H-1-benzopyrano[4,3-b]quinolin-6-one derivatives derivatives (3a-3l). The synthesized analogues **3a-3l** was evaluated their anti-cancer activity. 9,10-difluoro-6H-chromeno[4,3-b]quinolin-6-one **3c** was shown potent inhibition against colon cancer cells.

References

- Ajdini N, Leci O, Tabakovic I, Tabakovic K. Chemistry of coumarin, phase-transfer catalysis in the C-alkylation of 4-arylamino coumarins. Bull Soc Chim. 1984; 49: 495-500.
- Bairagi S, Bhosale A, Deodhar MN. Design, Synthesis and Evaluation of Schiff's Bases of 4-Chloro-3-coumarin aldehyde as Antimicrobial Agents. E-J Chem. 2009; 6: 759-62.
- Carmichael J, DeGraff WG, Gazdar AF, Minna JD, Mitchell

- JB. Evaluation of a tetrazolium-based semiautomated colorimetric assay: Assessment of chemosensitivity testing. *Cancer Res.* 1987; 47: 936-42.
- Geissman TA. The chemistry of flavonoid compounds. Oxford, Pergamon Press, 1962.
- Harborne JB. The Flavonoids. The advances in research since 1980. London, Chapman and Hall, 1988a.
- Harborne JB. The flavonoids, The advances in research since 1986. London, Chapman and Hall, 1988b.
- Hegab MI, Abdel-Fattah A-SM, Yousef NM, Nour HF, Mostafa AM, Ellithy M. Synthesis, X-ray structure, and pharmacological activity of some 6,6-disubstituted chromeno[4,3-*b*]- and chromeno-[3,4-*c*]-quinolines. *Arch Der Pharm.* 2007; 340: 396-403.
- Henkels KM, Turchi J. Cisplatin-induced apoptosis proceeds by caspase-3-dependent and -independent pathways in cisplatin-resistant and -sensitive human ovarian cancer cell lines. *Cancer Res.* 1999; 59: 3077-83.
- Koopman G, Reutelingsperger CP, Kuijten GA, Keehnen RM, Pals ST, van Oers MH. Annexin V for flow cytometric detection of phosphatidylserine expression on B cells undergoing apoptosis. *Blood* 1994; 84: 1415-20.
- Miri R, Motamedi R, Rezaei MR, Firuzi O, Javidnia A, Shafiee A. Design, synthesis and evaluation of cytotoxicity of novel chromeno[4,3-*b*]quinoline derivatives. *Arch Der Pharm.* 2011; 344: 111-18.
- Mulakayala N, Rambabu D, Rao RM, Chaitanya M, Kumar CS, Kalle AM, Krishna GR, Reddy CM, Rao MVB, Pal M. Ultrasound mediated catalyst free synthesis of 6H-1-benzopyrano [4, 3-*b*] quinolin-6-ones leading to novel quinoline derivatives: Their evaluation as potential anti-cancer agents *Bioorg Med Chem.* 2012; 20: 759-68.
- Pondugula SR, Dong H, Chen T. Phosphorylation and protein-protein interactions in PXR-mediated CYP3A repression. *Expert Opin Drug Metab Toxicol.* 2009; 5: 861-73.
- Pondugula SR, Mani S. Pregnane xenobiotic receptor in cancer pathogenesis and therapeutic response. *Cancer Lett.* 2013; 328: 1-9.
- Perin N, Uzelac L, Piantanida I, Karminski-Zamola G, Kralj M, Hranjec M. Novel biologically active nitro and amino substituted benzimidazo[1,2-*a*]quinolines. *Bioorg Med Chem.* 2011; 19: 6329-39.
- Rappa G, Shyam K, Lorico A, Fodstad O, Sartorelli AC. Structure-activity studies of novobiocin analogs as modulators of the cytotoxicity of etoposide (VP-16). *Oncol Res.* 2000; 12: 113-19.
- Robey RW, Medina-Perez WY, Nishiyama K, Lahusen T, Miyake K, Litman T, Senderowicz AM, Ross DD, Bates SE. Overexpression of the ATP-binding cassette half-transporter, ABCG2 (Mxr/BCrp/ABCP1), in flavopiridol-resistant human breast cancer cells. *Clin Cancer Res.* 2001; 7: 145-52.
- Tabakovic I, Grujic Z, Bejtovic Z. Electrochemical synthesis of heterocyclic compounds. XII. Anodic oxidation of catechol in the presence of nucleophiles. *J Heterocycl Chem.* 1983; 20: 635-38.
- Tabakovic K, Tabakovic I, Ajdini N, Leci O. A novel transformation of 4-arylamino coumarins to 6 H-1-benzopyrano[4,3-*b*]quinolin-6-ones under vilsmeier-haack conditions. *Synthesis* 1987; 3: 308-11.
- Thaisrivongs MN, Janakiraman KT, Chong PK, Tomich LA, Dolack SR, Turner JW, Strohbach JC, Lynn MM, Horng RR, Hinshaw KD. Structure-based design of novel HIV protease inhibitors: sulfonamide-containing 4-hydroxycoumarins and 4-hydroxy-2-pyrones as potent non-peptidic inhibitors. *J Med Chem.* 1996; 39: 2400-10.
- Vu AT, Campbell AN, Harris HA, Unwalla RJ, Manas ES, Mewshaw RE. Structure-based design of novel HIV protease inhibitors: Sulfonamide-containing 4-hydroxycoumarins and 4-hydroxy-2-pyrones as potent non-peptidic inhibitors. *Bioorg Med Chem Lett.* 2007; 17: 4053-56.
- Wu CP, Woodcock H, Hladky SB, Barrand MA. cGMP (guanosine 3',5'-cyclic monophosphate) transport across human erythrocyte membranes. *Biochem Pharmacol.* 2005; 69: 1257-62.
- Yang ED, Zhao YN, Zhang K, Mack P. Daphnetin, one of coumarin derivatives, is a protein kinase inhibitor. *Biochem Biophys Res Commun.* 1999; 260: 682-85.

Author Info

Hai-Feng Guo (Principal contact) e-mail: guohaifeng07@gmail.com;